

KfK 3183
DESY 81-021
Mai 1981

**Measurement of $e^+ e^- \rightarrow e^+ e^-$
and $e^+ e^- \rightarrow \gamma\gamma$ at Energies
up to 36.7 GeV**

CELLO-Collaboration
Institut für Kern- und Teilchenphysik

Kernforschungszentrum Karlsruhe

KERNFORSCHUNGSZENTRUM KARLSRUHE
Institut für Kern- und Teilchenphysik

KfK 3183

DESY 81-021

Measurement of $e^+e^- \rightarrow e^+e^-$ and $e^+e^- \rightarrow \gamma\gamma$ at Energies
up to 36.7 GeV

CELLO-Collaboration

Kernforschungszentrum Karlsruhe GmbH, Karlsruhe

**Als Manuskript vervielfältigt
Für diesen Bericht behalten wir uns alle Rechte vor**

**Kernforschungszentrum Karlsruhe GmbH
ISSN 0303-4003**

Abstract

The differential cross sections of the reactions $e^+e^- \rightarrow e^+e^-$ and $e^+e^- \rightarrow \gamma\gamma$ are measured at energies between 33.0 and 36.7 GeV. The results agree with the predictions of quantum electrodynamics. A comparison with the standard model of electroweak interaction yields $\sin^2\theta_W = 0.25 \pm 0.13$.

Messung von $e^+e^- \rightarrow e^+e^-$ und $e^+e^- \rightarrow \gamma\gamma$ bei Energien bis zu 36.7 GeV

Zusammenfassung

Die differentiellen Wirkungsquerschnitte der Reaktionen $e^+e^- \rightarrow e^+e^-$ und $e^+e^- \rightarrow \gamma\gamma$ wurden bei Energien zwischen 33.0 und 36.7 GeV gemessen. Die Ergebnisse stimmen mit den Vorhersagen der Quantenelektrodynamik überein. Ein Vergleich mit dem Standardmodell der elektroschwachen Wechselwirkung liefert $\sin^2\theta_W = 0.25 \pm 0.13$.

Measurement of $e^+e^- \rightarrow e^+e^-$ and $e^+e^- \rightarrow \gamma\gamma$ at Energies up to 36.7 GeV

CELLO-Collaboration

H.-J. Behrend, Ch. Chen¹, J. Field, U. Gümpel, V. Schröder, H. Sindt
Deutsches Elektronen-Synchrotron, Hamburg, Federal Republic of Germany

W.-D. Apel, J. Bodenkamp, D. Chrobaczek, J. Engler, D.C. Fries,
G. Flügge, G. Hopp, H. Müller, F. Mönnig, H. Randoll, G. Schmidt,
H. Schneider

Kernforschungszentrum Karlsruhe and Universität Karlsruhe,
Federal Republic of Germany

W. de Boer, G. Buschhorn, G. Grindhammer, P. Grosse-Wiesmann,
B. Gunderson, C. Kiesling, R. Kotthaus, U. Kruse², H. Lierl, D. Lüers,
T. Meyer, L. Moss, H. Oberlack, P. Schacht, M.-J. Schachter,
A. Snyder, H. Steiner³

Max-Planck-Institut für Physik und Astrophysik, München,
Federal Republic of Germany

G. Carnesecchi, A. Cordier, M. Davier, D. Fournier, J.F. Grivaz,
J. Haissinski, V. Journé, A. Klarsfeld, M. Cohen, F. Laplanche,
F. Le Diberder, U. Mallik, J.-J. Veillet, A. Weitsch
Laboratoire de l'Accélérateur Linéaire, Orsay, France

R. George, M. Goldberg, B. Grossetête, F. Kapusta, F. Kovacs,
G. London, L. Poggioli, M. Rivoal
Laboratoire de la Physique Nucléaire et Hautes Energies,
Paris, France

R. Aleksan, J. Bouchez, G. Cozzika, Y. Ducros, A. Gaidot, J. Pamela,
J.P. Pansart, F. Pierre
Centre d'Etudes Nucléaires, Saclay, France

¹ Visitor from Institute of High Energy Physics, Chinese Academy
of Science, Peking, People's Republic of China

² Visitor from University of Illinois, Urbana, USA

³ Alexander von Humboldt Foundation Senior American Scientist,
University of California, Berkeley, Ca., USA

The measurement of the production of lepton and photon pairs in high energy e^+e^- reactions provides a stringent test of the validity of quantum electrodynamics (QED) at large momentum transfer¹⁾. In addition, at highest accessible PETRA energies weak neutral current effects get increasingly important for Bhabha scattering. This allows to test weak interaction phenomena in purely leptonic processes.

We report on a measurement of the reaction

$$e^+e^- \rightarrow e^+e^- \text{ (Bhabha scattering)} \quad (1)$$

and

$$e^+e^- \rightarrow \gamma\gamma \quad (2)$$

at CM energies between 33.0 and 36.7 GeV. The experiment was performed using the CELLO detector at the e^+e^- storage ring PETRA.

The detector has been described previously²⁾. The detector components essentially used in the analysis will briefly be presented.

The central detector consists of cylindrical drift and proportional chambers in a solenoidal field of 1.3 T. The transverse momentum resolution is $\sigma_{p_{\perp}}/p_{\perp} = 0.02 p_{\perp}$ (p_{\perp} in GeV), the angular precisions are $\Delta\theta = 2$ mrad from the proportional chamber cathode strips and $\Delta\phi = 3$ mrad from the drift chambers. These numbers include the knowledge on the interaction vertex.

The lead liquid argon system provides electromagnetic shower recognition in 96% of the solid angle. The central calorimeter consists of 16 modules placed outside the thin superconducting coil ($0.48 X_0$) in the angular range $|\cos \theta| < 0.88$. The endcap calorimeter consists of four modules, two on each side. It covers the angular range $0.91 \leq |\cos \theta| \leq 0.99$.

Each calorimeter module has a thickness of 20 (endcap 21) radiation lengths. Readout strips in different directions (central: longitudinal, perpendicular, and 45° , endcap: horizontal, vertical and circular) allow for shower reconstruction with a precision of typically 4 mrad. The energy resolution follows $\sigma_E/E = 0.13/\sqrt{E}$ (including material in front of the detector) up to highest PETRA energies. This results in a (measured) resolution of $3.2\% \pm 0.7\%$ at $E = 17 \text{ GeV}^2$). One out of the 16 central modules was not operational during data taking.

The present analysis is based on an integrated luminosity of 3.8 pb^{-1} taken between May and November 1980. QED events were recorded on tape if either of the following conditions was fulfilled:

- more than 6 GeV of energy in the calorimeter
- at least two tracks separated by more than 45° in the central detector
- at least one track in the central detector and 3 GeV in the calorimeter.

The efficiency of the combined triggers was larger than 99%.

All events with an energy of more than $2 \times 3 \text{ GeV}$ colinear within 45° in the central calorimeter were processed through a track reconstruction program. Candidate samples for the two reactions under study were selected if they fulfilled the following criteria:

reaction (1): at least two tracks in the central detector

reaction (2): the remaining sample with an increased energy cut of $2 \times 10 \text{ GeV}$ to get comparable data reduction.

These candidate samples were processed through a shower reconstruction program. To restore the simple topology of QED events which was partly destroyed in the beam pipe and in the synchrotron radiation tin shield (total of 0.15 radiation lengths) an algorithm was applied to form charged and neutral clusters.

Charged tracks, their correlated showers and other showers with relative angles less than 200 mrad were combined to form charged clusters. The remaining showers were grouped into neutral clusters, again within 200 mrad. The axis for charged clusters was calculated as the momentum weighted average of the direction of charged particles. In neutral clusters the corresponding weighted average of shower directions was taken.

Candidate events for reactions (1) and (2) were accepted if they had at least two clusters colinear within 250 mrad and a neutral energy of more than 1/3 beam energy in at least one of those clusters. The angular range in the central calorimeter was restricted to $|\cos \theta| < 0.86$ to exclude edge effects. Events with charged tracks in both colinear clusters were attributed to reaction (1), the others to reaction (2).

In 1.2% of the events of class (1) no unambiguous charge assignment could be obtained. These events were subdivided into forward and backward scattering according to the measured distribution of events with charge determination. All events with $\cos \theta < 0.4$ and a large fraction of the other events were scanned visually. A residual background from hadronic and τ events (0.2%) was removed. Wrong charge assignment due to pattern recognition problems was corrected (0.1%). A small fraction of wrongly assigned $\gamma\gamma$ events was moved into class (2) ($< 0.1\%$).

The total detection efficiency for reaction (1) was $94 \pm 2\%$. The losses were due to trigger inefficiencies (1%) and preselection cuts on the calorimeter energy (5%), which were partly due to edge effects between the liquid argon modules.

For reaction (2) the candidate sample was entirely scanned by visual inspection. Few events ($\approx 2\%$) had to be attributed to reaction (1) because one of the electrons was not found by the pattern recognition program. The probability to lose $\gamma\gamma$ events due to double γ conversion was estimated from single conversion and corrected for (less than 2%). The overall efficiency to detect $\gamma\gamma$ events was $70\% \pm 10\%$. This number was checked by imposing the selection criteria of reaction (2) on events of re-

action (1) neglecting charged tracks.

Events in the endcap region were selected by requiring at least 30% of the beam energy in each of 2 back-to-back endcap calorimeters and no energy in the remaining calorimeter. (Only ~20% of the data were used in the analysis.) The geometrical acceptance of the endcap calorimeters imposed an acolinearity cut of ~150 mrad on the selected events. Part of the event sample was checked by visual inspection. All data were processed through a shower reconstruction program. Cluster algorithms similar to those for the central QED events were applied to pick up associated neutral energy. The $\gamma\gamma$ events (0.7%) were removed by statistical subtraction. The remaining e^+e^- events were corrected for azimuthal losses (6.3%) and losses due to the energy cuts (1.6%). The cross section thus obtained has a statistical error of 2.9% (including uncertainties of the corrections) and a systematic error of 3.1%.

Fig.1 shows the resulting differential cross section for Bhabha events. The data was corrected for radiative effects in order α^3 and hadronic vacuum polarisation³⁾. The expectation from QED is indicated in the figure. The relative normalization of the endcap and central detector agrees within 0.3%.

To determine quantitative limits on the validity of QED the reaction amplitude is usually modified by introducing form factors⁴⁾ $F(q^2)$ and $F(s)$

$$\frac{d\sigma}{d\Omega} = \frac{\alpha^2}{4s} \left| \frac{10+4x+2x^2}{(1-x)^2} F^2(q^2) - 2 \frac{(1+x)^2}{1-x} F(q^2)F(s) + (1+x^2)F^2(s) \right| \quad (3)$$

where s is the centre of mass energy squared and $q^2 = \frac{s}{2}(x-1)$;
 $x = \cos \theta$.

The formfactors can be parametrized as

$$F(q^2) = 1 \pm \frac{q^2}{q^2 - \Lambda_{\pm}^2} \quad F(s) = 1 \pm \frac{s}{s - \Lambda_{\pm}^2}$$

To extract values for the cut off parameters Λ it was assumed that formfactors do not affect the endcap region $0.96 < \cos < 0.98$. If we further assume statistical errors only we get the following limits for Λ_{\pm} :

$$\Lambda_{+} > 83 \text{ GeV} \quad (95\% \text{ C.L.})$$

$$\Lambda_{-} > 155 \text{ GeV} \quad (95\% \text{ C.L.})$$

Allowing for an additional systematic uncertainty in the relative normalization between central and endcap calorimeter (3.1%) we get: $\Lambda_{+} > 74 \text{ GeV}$, $\Lambda_{-} > 150 \text{ GeV}$ (95% C.L.). Our values agree well with those of the other PETRA groups (Table 1a).

Deviations from the QED prediction are expected from weak neutral current effects. Including γ - Z^0 interference the Bhabha cross section depends on the vector and axial weak coupling constants g_V and g_A and the Z^0 mass M_{Z^0} ⁵⁾. In the standard $SU(2) \times U(1)$ model⁶⁾ they are determined by one single parameter, $\sin^2 \theta_w$:

$$M_Z = \frac{37.4}{\sin \theta_w \cos \theta_w}$$

$$g_A^2 = \frac{1}{4}$$

$$g_V^2 = \frac{1}{4} (1 - 4 \sin^2 \theta_w)^2.$$

The predictions for the cross section of reaction (1) for various values of $\sin^2 \theta_w$ are indicated in fig.2.

If we take into account statistical errors only

a fit to the data yields the following values

$$\sin^2\theta_w = 0.25 \pm 0.13$$

$$0.01 < \sin^2\theta < 0.49 \quad (95\% \text{ C.L.})$$

The 95% C.L. limits change to $\sin^2\theta_w < 0.50$ if we allow for the additional systematic uncertainty between endcap and central calorimeter normalization.

Fig.3 shows the angular distribution for events of reaction (2) in the central calorimeter. Data agree well with the QED predictions normalized to reaction (1).

To establish quantitative limits the cross section can again be modified by

$$\frac{d\sigma}{d\Omega} = \frac{\alpha^2(1+x^2)}{s(1-x^2)} \left| 1 \pm \frac{s^2}{2\Lambda_{\pm}^4} (1-x^2) \right| \quad (4)$$

$\Lambda_{\pm} = M_{e^{\pm}}/\lambda$ can be regarded as the ratio of the mass of a hypothetical heavy electron mediating the reaction and its coupling constant λ^7).

A best fit to our data yields

$$\Lambda_{+} > 43 \text{ GeV} \quad (95\% \text{ C.L.})$$

$$\Lambda_{-} > 48 \text{ GeV} \quad (95\% \text{ C.L.})$$

in good agreement with the other PETRA groups (Table 1b).

In conclusion a study of e^+e^- and $\gamma\gamma$ production was performed up to highest PETRA energies.

The measurements show no deviation from QED indicating that the electron is structureless down to distances of about 10^{-16} cm. Data start to be sensitive to weak neutral current effects and yield a value for the mixing angle in the standard model, $\sin^2\theta_w = 0.25 \pm 0.13$.

Acknowledgement

We are indebted to the PETRA machine group and the DESY computer centre for their excellent support during the experiment. We acknowledge the invaluable effort of all engineers and technicians of the collaborating institutions in construction and maintenance of the apparatus. The visiting groups wish to thank the DESY directorate for the support and kind hospitality extended to them. This work was partly supported by the Bundesministerium für Forschung und Technologie.

Table 1a: Cut-off parameters for $e^+e^- \rightarrow e^+e^-$ (8).
All numbers are 95% C.L. lower limits

Experiment	Λ_+ (Gev)	Λ_- (GeV)
CELLO	83	155
JADE	112	106
MARK J	91	142
PLUTO	80	234
TASSO	150	136

Table 1b: Cut-off parameters for $e^+e^- \rightarrow \gamma\gamma$ (8).
All numbers are 95% C.L. lower limits

Experiment	Λ_+ (GeV)	Λ_- (GeV)
CELLO	43	48
JADE	47	44
MARK J	55	38
PLUTO	46	--
TASSO	34	42

References

- 1) JADE Collaboration, W.Bartel et al., Phys.Lett. 92B (1980) 206,
99B (1981) 281 and DESY Report 81-015 (March 81)
MARK J Collaboration, D.P.Barber et al., Phys.Rev.Lett. 42
(1979) 1110, 43 (1979) 1915 and
Phys.Lett. 95B (1980) 149
and RWTH Aachen preprint PITHA 81/7 (1981)
PLUTO Collaboration, Ch.Berger et al., Z.f.Physik C4(1980)269, C7(1981)289
and Phys.Lett. 94B (1980) 87
TASSO Collaboration, R.Brandelik et al., Phys.Lett. 92B (1980)199
and 94B (1980) 259
- 2) CELLO Collaboration, H.-J. Behrend et al., Phys.Scripta 23
(1981) 610
- 3) F.A.Berends, K.J.F.Gaemers and R.Gastmans, Nucl.Phys. B57
(1973) 381 and B63 (1973) 381 and B68 (1979) 541
F.A.Berends and G.J.Komen, Phys.Lett. 63B (1976) 432
- 4) H.Salecker, Z.für Naturforschung 8a (1953) 16 and 10a (1955)349
S.D.Drell, Ann.Phys. 4 (1958) 75
T.D.Lee and G.G.Wick, Phys.Rev. D2 (1970) 1033
- 5) R.Budny, Phys.Lett. 55B (1975) 227
- 6) S.L.Glashow, Nucl.Phys. 22 (1961) 579
S.Weinberg, Phys.Rev.Lett. 19 (1967) 1264
A.Salam, Proc. 8th Nobel Symposium, Stockholm (1968)
- 7) A.Litke, Harvard University, Ph.D.Thesis (unpublished) 1970
- 8) A.Böhm, RWTH Aachen preprint PITHA 80/9 (1980), Invited Talk
at the XXth Int.Conf. on High Energy Physics, Madison, 1980,
to be published

Figure Captions

Fig.1: Differential cross section of the reaction $e^+e^- \rightarrow e^+e^-$ in the central detector and endcap calorimeter range. Only statistical errors are plotted. The QED prediction (full curve) is normalized to the endcap points.

Fig.2: Relative deviation of the measured cross section from QED prediction. Errors are statistical only. The expectation for different values of $\sin^2\theta_w$ is indicated.

Fig.3: Differential cross section of the reaction $e^+e^- \rightarrow \gamma\gamma$ compared to the QED prediction. Only statistical errors are plotted.

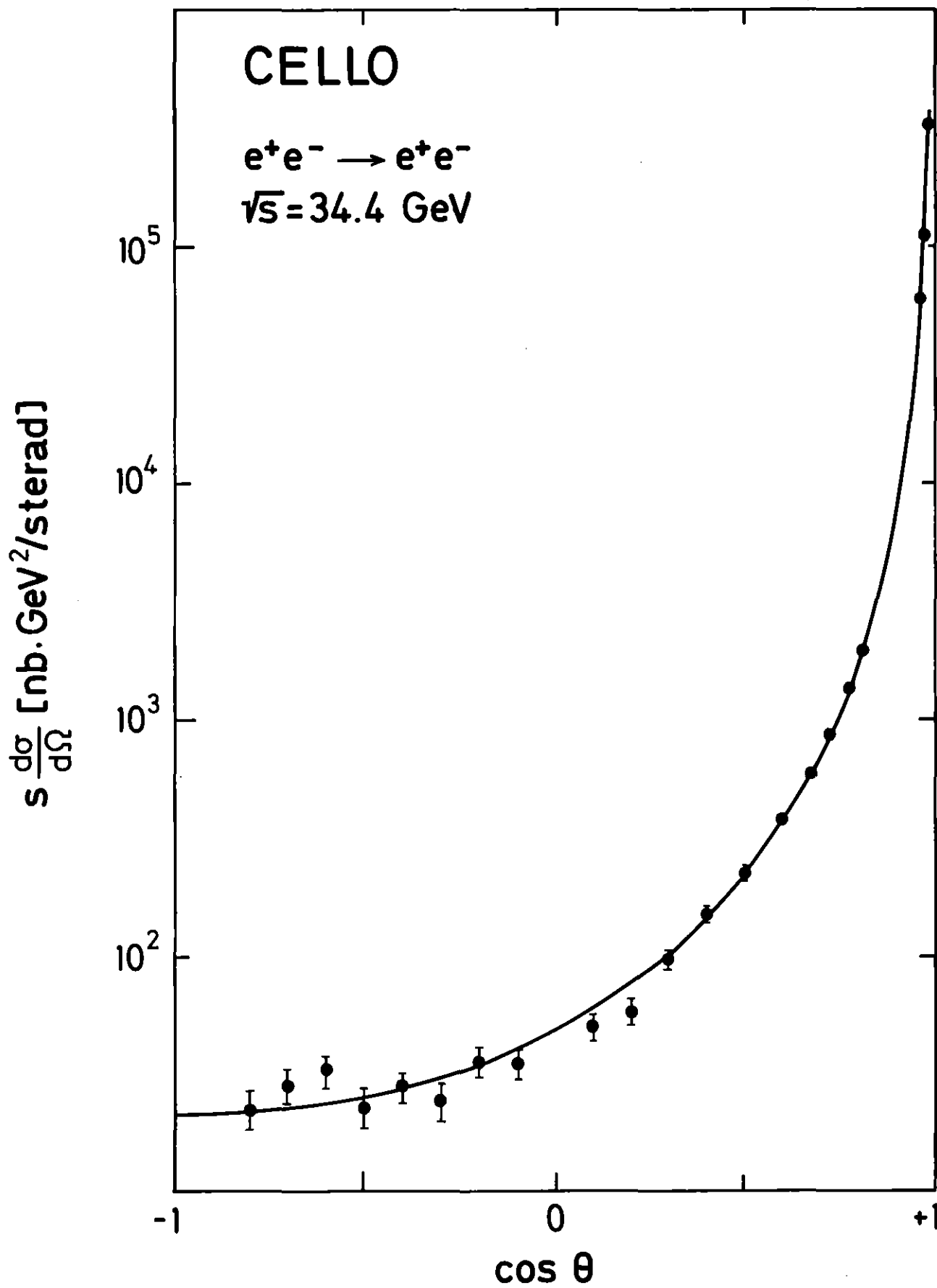


Fig.1

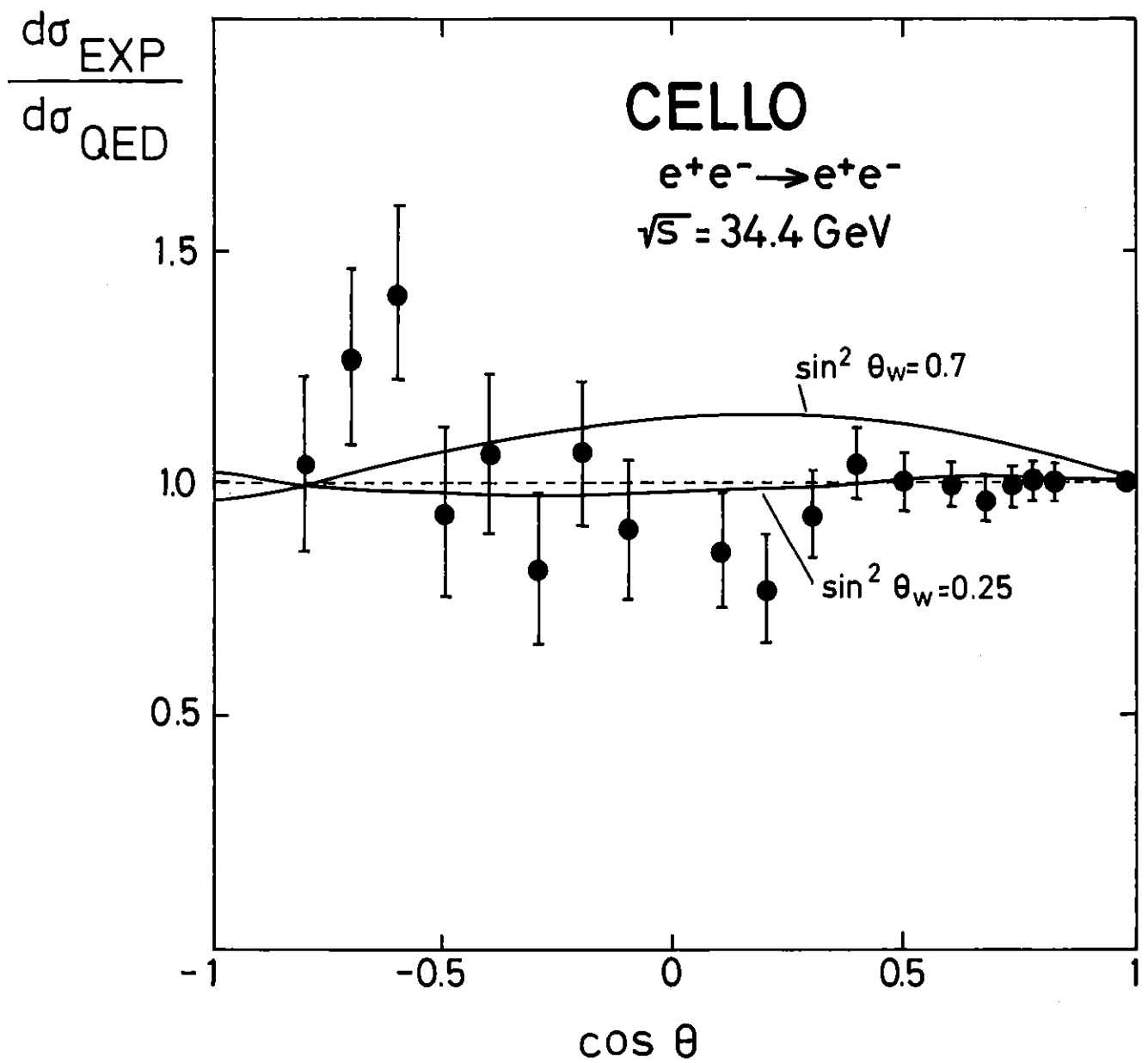


Fig.2

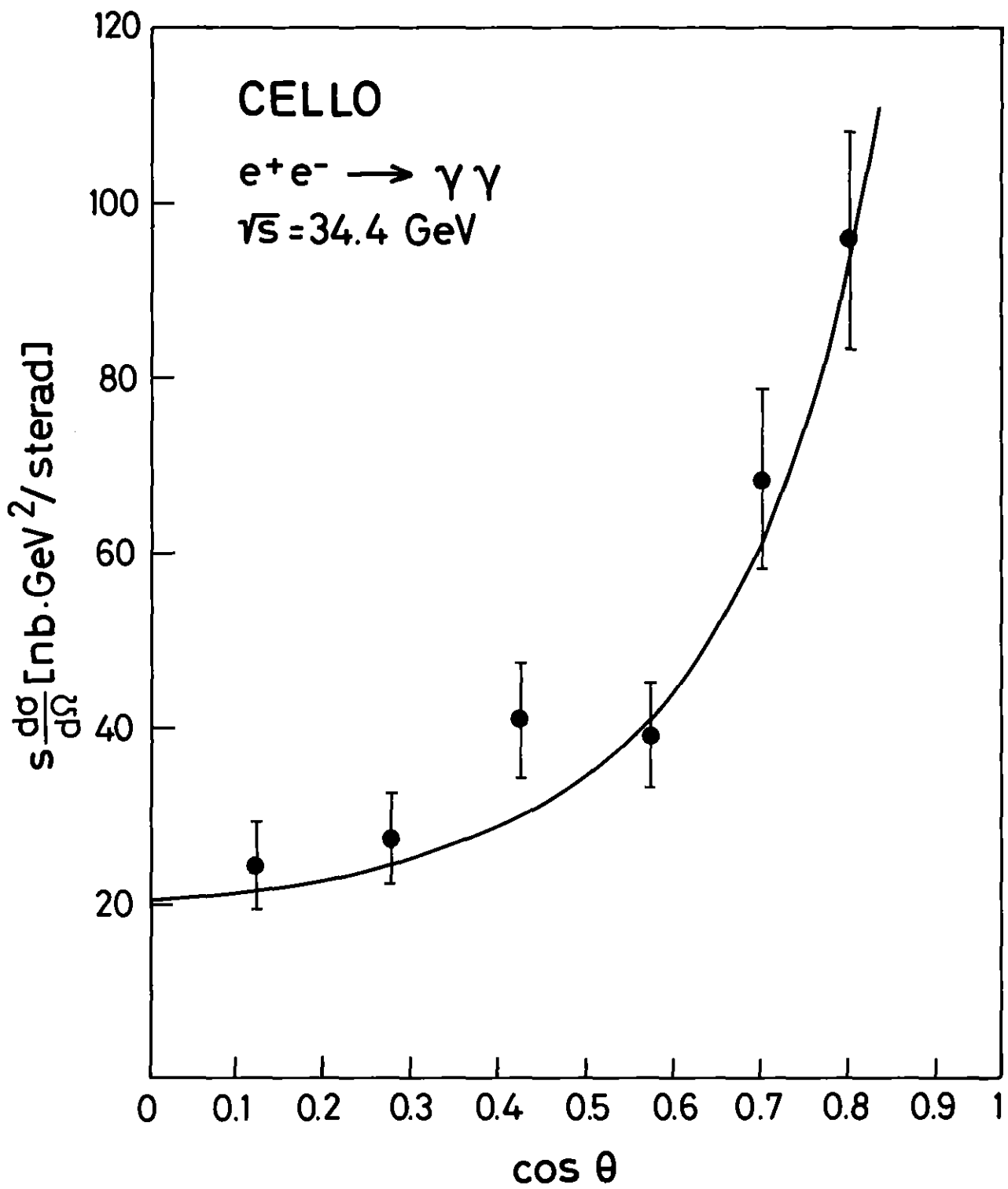


Fig.3